Steel and Composite Structures, *Vol. 18, No. 5 (2015) 1119-1127*
DOI: http://dx.doi.org/10.12989/scs.2015.18.5.1119

Modeling and simulation of partially delaminated composite beams

A. Mahieddine [*1], M. Ouali [2a] and A. Mazouz [1b]

[1] *Energy and smart systems laboratory, Khemis Miliana University, 44225, Algeria*
[2] *Structures laboratory, Saad Dahleb University, 09000, Algeria*

(*Received April 24, 2014, Revised September 26, 2014, Accepted November 07, 2014*)

Abstract. A finite-element model for beams with partially delaminated layers is used to investigate their behavior. In this formulation account is taken of lateral strains and the first-order shear deformation theory is used. Both displacement continuity and force equilibrium conditions are imposed between the regions with and without delamination. Numerical results of the present model are presented and its performance is evaluated for static and dynamic problems.

Keywords: delamination; beam; shear deformation theory; damage; composite structure

1. Introduction

The mechanical properties of composite materials may degrade severely in the presence of damage. Delamination is a frequently encountered mode of internal damage and is one of the most prevalent life-limiting failure modes in laminated composite structure.

Many researchers had been studying the effect of Delamination. Mahieddine *et al*. (2010) present a mathematical model for analysis of delaminated beams with integrated piezoelectric actuators. A simplified analysis of dynamic delamination in composites is presented by Corigliano *et al*. (2006). The effect of delamination resistance on fatigue crack growth behavior of composite laminates is studied by Zhang *et al*. (2012). Coronado *et al*. (2012) analysed the influence of temperature on the process of mode-I delamination in a carbon fibre reinforced epoxy material under static and fatigue loadings. Zhao *et al*. (2013) established an analysis method to predict delamination and/or filler crack of out-of-plane woven composite joints using cohesive elements. The actions of typical parameters about material, interfacial and computational aspects in definition of cohesive element are depicted and a parameter model is proposed. For the prediction of delamination initiation and growth, a method based on a damage mechanics approach by adopting softening relationships between tractions and separations is used to simulate the delamination by Benzerga *et al*. (2012). Lee *et al*. (2002) studied a composite beam with arbitrary

∗Corresponding author, Ph.D., E-mail: mahieddine.ali@gmail.com
[a] Professor, E-mail: oualimohammed@yahoo.fr
[b] Ph.D., E-mail: mazouz.amel@yahoo.fr

http://www.techno-press.org/?journal=scs&subpage=8 ISSN: 1229-9367 (Print), 1598-6233 (Online)

lateral and longitudinal multiple delamination. Finite element methods have been developed using the layerwise theory by Kim *et al*. (2003). An improved analytical model for delamination in composite beams, using a second-order shear-thickness deformation displacement field, was introduced by Hamed *et al*. (2006). A simplified hinge for load introduction in composite delamination and adhesive tests using beam-type specimens has been presented by Renart *et al*. (2011). The proposed solution does not include adhe-sive joints susceptible of failure during the tests. Brandt (1998) introduced a mechanical hinge to overcome all these problems. This hinge includes a metallic fastener box with a slot where the bending beam of the specimen is fitted and mechanically adjusted. Sjögren and Asp (2002) presents a study of delamination growth in HTA/6376C carbon fibre/epoxy laminates. Tests were conducted under Mode I, Mode II and mixed-mode static and fatigue loading at both ambient conditions and elevated temperature. An investigation on dynamic delamination problems under steady-state crack growth is proposed by Greco and Lonetti (2009). Through the thickness delamination phenomena in unidirectional composite laminates are analyzed in the context of the interface methodology, based on the combination of shear deformable beams and interface elements. Prokić *et al*. (2014) developed a computer program for the determination of geometrical and material properties of composite thin-walled beams with arbitrary open cross-section and any arbitrary laminate stacking sequence. Bending behavior of reinforced concrete slabs encased over shallow I-sections at different levels of compression heads were investigated by Gőrkem and Hűsem (2013).

A finite-element model is developed to investigate the effects of delamination of a beam layers. The present model takes into account the lateral strains which are often neglected in the conventional models of beams. The principal advantage of the element is that it allows the modeling of delamination anywhere in the structure. The region without delamination is modeled to carry constant peel and shear stresses; while the region with delamination is modeled by assuming that there is no peel and shear stress transfer between the top and bottom layers. The accuracy of the approach is verified by comparing results with previously published data.

2. Finite element formulation

Considering the first-order shear deformation theory for a laminated composite beam, the axial and the transverse displacement field are expressed by

$$\begin{aligned} U^{(i)}(x,y,z,t) &= u^{(i)}(x,t) - z\theta_y^{(i)}(x,t) \\ W^{(i)}(x,y,z,t) &= w^{(i)}(x,t) \end{aligned} \tag{1}$$

where $U^{(i)}$ and $W^{(i)}$ are axial and transverse displacement. $i = T, B$ represent the top and bottom layers.

The strain relations for each of the sublaminates associated with the displacement field are given by

$$\begin{aligned} \varepsilon_x^{(i)} &= U_{,x}^{(i)} \\ \gamma_{xz}^{(i)} &= U_{,z}^{(i)} + W_{,x}^{(i)} \end{aligned} \tag{2}$$

Using Eq. (1), the strain relations can be given by

$$\begin{aligned} \varepsilon_x^{(i)} &= u_{,x}^{(i)} - z\theta_{y,x}^{(i)} \\ \gamma_{xz}^{(i)} &= -\theta_y^{(i)} + w_{,x}^{(i)} \end{aligned} \tag{3}$$

where $(\bullet)_{,x}$ denotes differentiation with respect to x.

The stress for each layer is given by

$$\begin{pmatrix} \sigma_x \\ \sigma_y \\ \tau_{xy} \\ \tau_{xz} \\ \tau_{yz} \end{pmatrix} = \begin{pmatrix} C_{11} & C_{12} & 0 & 0 & 0 \\ C_{21} & C_{22} & 0 & 0 & 0 \\ 0 & 0 & C_{44} & 0 & 0 \\ 0 & 0 & 0 & C_{55} & 0 \\ 0 & 0 & 0 & 0 & C_{66} \end{pmatrix} \cdot \begin{pmatrix} \varepsilon_x \\ \varepsilon_y \\ 2\varepsilon_{xy} \\ 2\varepsilon_{xz} \\ 2\varepsilon_{yz} \end{pmatrix} \tag{4}$$

The constitutive relations, which neglect the thermal effects, are given by

$$\begin{Bmatrix} \sigma_x^{(i)} \\ \tau_{xz}^{(i)} \end{Bmatrix} = \begin{bmatrix} \widetilde{C}_{11}^{(i)} & 0 \\ 0 & \widetilde{C}_{55}^{(i)} \end{bmatrix} \begin{Bmatrix} \varepsilon_x^{(i)} \\ \gamma_{xz}^{(i)} \end{Bmatrix} \tag{5}$$

where $\sigma_x^{(i)}$ is the normal stress, $\varepsilon_x^{(i)}$ is the normal strain, $\tau_{xz}^{(i)}$ is the shear stress and $\gamma_{xz}^{(i)}$ is the shear strain.

The expression for $\widetilde{C}_{11}^{(i)}$ are as follows

$$\begin{aligned} \widetilde{C}_{11}^{(i)} &= C_{11}^{(i)} - \frac{C_{12}^{(i)}}{C_{22}^{(i)}} \\ \widetilde{C}_{55}^{(i)} &= C_{55}^{(i)} \end{aligned} \tag{6}$$

The strain energy (E_p) and the kinetic energy (E_c) are given by

$$E_c = \frac{1}{2} \int_{\Omega^{(i)}} \rho^{(i)} \cdot \left(\dot{U}^{(i)2} + \dot{W}^{(i)2} \right) \cdot d\Omega^{(i)} \tag{7}$$

$$E_p = \frac{1}{2} \int_{\Omega^{(i)}} \left(\sigma_x^{(i)} \varepsilon_x^{(i)} + \tau_{xz}^{(i)} \gamma_{xz}^{(i)} \right) \cdot d\Omega^{(i)} \tag{8}$$

where (.) denotes temporal derivatives, $\Omega^{(i)}$ is the volume of the layer.

In order to perform a finite element formulation, the unknown functions $u^{(i)}(x,t)$, $w^{(i)}(x,t)$ and $\theta_y^{(i)}(x,t)$ are represented by piecewise interpolation polynomials

$$\begin{Bmatrix} u^{(i)} & w^{(i)} & \theta_y^{(i)} \end{Bmatrix} = \begin{bmatrix} N^{(i)} \end{bmatrix} \begin{Bmatrix} q^{(i)} \end{Bmatrix}$$

where

$$\left[N^{(i)}\right]=\begin{bmatrix} N_1 & 0 & 0 & N_2 & 0 & 0 \\ 0 & N_3 & N_4 & 0 & N_5 & N_6 \\ 0 & N_7 & N_8 & 0 & N_9 & N_{10} \end{bmatrix}=\begin{bmatrix} N_u^{(i)} \\ N_w^{(i)} \\ N_\theta^{(i)} \end{bmatrix}$$

and

$$N_1=1-\xi; \quad N_2=2\xi^3-3\xi^2+1; \quad N_3=L_e\xi(\xi-1)^2; \quad N_4=\xi; \quad N_5=\xi^2(3-2\xi);$$
$$N_6=L_e\xi^2(\xi-1); \quad N_7=\frac{6}{L_e}(\xi^2-\xi); \quad N_8=(3\xi^2-4\xi+1); \quad N_9=\frac{6}{L_e}(-\xi^2+\xi); \quad N_{10}=3\xi^2-2\xi$$

where $\xi=\dfrac{x}{L_e}$

Introducing a nodal parameters $\{q\}$ and by substitution of polynomial approximations of the unknown functions into Eqs. (5) and (6), the strain energy and kinetic energy can be written as

$$E_p=\frac{1}{2}\left\{q^{(i)}\right\}^T\cdot\left[K^{(i)}\right]\cdot\left\{q^{(i)}\right\} \tag{9}$$

$$E_c=\frac{1}{2}\left\{\dot{q}^{(i)}\right\}^T\cdot\left[M^{(i)}\right]\cdot\left\{\dot{q}^{(i)}\right\} \tag{10}$$

where the stiffness and mass matrices are given by

$$\begin{aligned}\left[K^{(i)}\right]=\int_{\Omega^{(i)}}\Bigg[&\widetilde{C}_{11}^{(i)}\left(\left[\frac{dN_u^{(i)}}{\partial x}\right]^t\left[\frac{dN_u^{(i)}}{\partial x}\right]+z^2\left[\frac{dN_\theta^{(i)}}{\partial x}\right]^t\left[\frac{dN_\theta^{(i)}}{\partial x}\right]-2z\left[\frac{dN_u^{(i)}}{\partial x}\right]^t\left[\frac{dN_\theta^{(i)}}{\partial x}\right]\right)\\&+\widetilde{C}_{55}^{(i)}\left[\left(\left[\frac{dN_w^{(i)}}{\partial x}\right]-\left[N_\theta^{(i)}\right]\right)^t\left(\left[\frac{dN_w^{(i)}}{\partial x}\right]-\left[N_\theta^{(i)}\right]\right)\right]\Bigg]d\Omega^{(i)}\end{aligned} \tag{11}$$

$$\left[M^{(i)}\right]=\rho^{(i)}\int_{\Omega^{(i)}}\left(\left[N_u^{(i)}\right]^t\left[N_u^{(i)}\right]+\left[N_w^{(i)}\right]^t\left[N_w^{(i)}\right]+z^2\left[N_\theta^{(i)}\right]^t\left[N_\theta^{(i)}\right]-2z\left[N_u^{(i)}\right]^t\left[N_\theta^{(i)}\right]\right)d\Omega^{(i)} \tag{12}$$

Applying Hamilton's principle, the governing differential equation expressed in global coordinates is obtained and can be written as

$$[M]\{\ddot{q}\}+[K]\{q\}=\{F\} \tag{13}$$

The elements in the delaminated region and the region without delamination are derived separately and all the variables in the displacement fields are independent.

The region without delamination is modeled by assuming that there is no peel and shear stress transfer between the top and bottom layers. Moreover, in the interfaces between the regions with and without delamination, both displacements and forces continuity conditions are imposed.

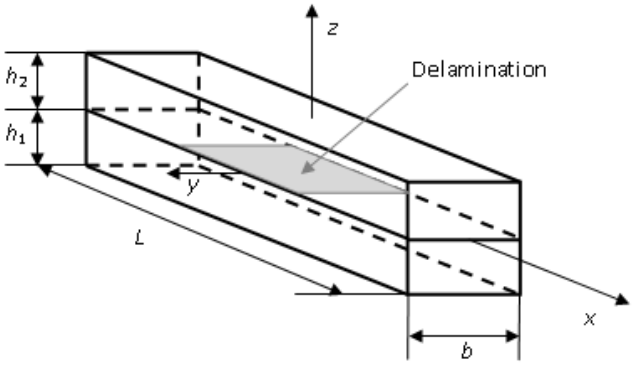

Fig. 1 Model of delaminated beam

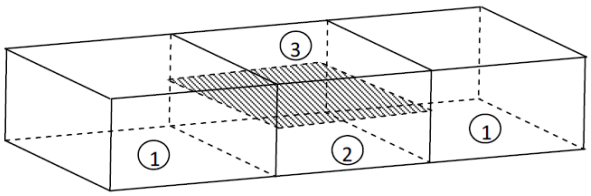

Fig. 2 Zones of delaminated beam

Table 1 Material parameters used in calculation

C_{11} [10^{10} N/m^2]	16.6
C_{12} [10^{10} N/m^2]	63.9
C_{13} [10^{10} N/m^2]	63.9
C_{33} [10^{10} N/m^2]	16.6
C_{44} [10^{10} N/m^2]	79.6
C_{66} [10^{10} N/m^2]	79.6
ρ [kg/m^3]	2330

The Beam is divided into three zones as shown in Fig. 2.
The constraint equations imposed are

$$\begin{aligned} w_2 &= w_1 \quad w_3 = w_1 \\ \theta_{y2} &= \theta_{y1} \quad \theta_{y3} = \theta_{y1} \end{aligned} \tag{14}$$

3. Results and discussions

In order to verify an accuracy of the finite elements model based on the formulation presented above, a beam with delamination between the top and the bottom layers was considered.

The beam's length, width and thickness are L = 0.4 m, b = 0.03 m and h = 0.01 m, a uniformly distributed load of 10^3 Nm^{-2} is applied. The parameters of the beam used in calculations are listed in Table 1.

For a clamped-free beam, the delamination length is chosen to be $L_d = \frac{1}{3}L$ located in the middle of the beam. The deflections computed by the present model are compared with those obtained by the use of an analytical model Mahieddine *et al*. (2010). The results are presented in Table 2. The results show good agreement between the values obtained with the two approaches.

Figs. 3 and 4 show the deflection field and the axial displacement field computed by this model for a clamped-free beam. Fig. 5 shows the stress field for the clamped-free beam.

Table 2 Deflections for the clamped-free beam

x [m]	w [m] from analytic model	w [m] from present model	Error
0.000000	0.000000	0.000000	0.000000
0.033333	-2.216622 e-4	-2.216622 e-4	4.729826 e-11
0.066667	-8.378124 e-4	-8.378124 e-4	4.949883 e-11
0.100000	-1.780080 e-3	-1.780080 e-3	5.182010 e-11
0.133333	-2.986606 e-3	-2.986606 e-3	5.420637 e-11
0.166667	-4.402042 e-3	-4.402042 e-3	5.656910 e-11
0.200000	-5.977553 e-3	-5.977553 e-3	5.876678 e-11
0.233333	-7.670813 e-3	-7.670813 e-3	6.087850 e-11
0.266667	-9.446009 e-3	-9.446009 e-3	6.291718 e-11
0.300000	-1.127384 e-2	-1.127384 e-2	6.488764 e-11
0.333333	-1.313152 e-2	-1.313152 e-2	6.669922 e-11
0.366667	-1.500276 e-2	-1.500276 e-2	6.825461 e-11
0.400000	-1.687780 e-2	-1.687780 e-2	6.941856 e-11

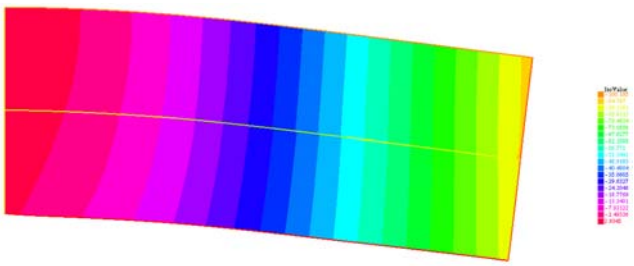

Fig. 3 Deflection field of the clamped-free beam

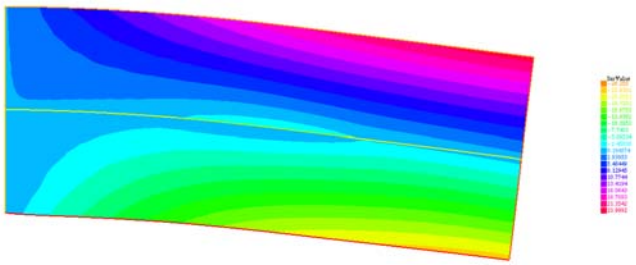

Fig. 4 Axial displacement of the clamped-free beam

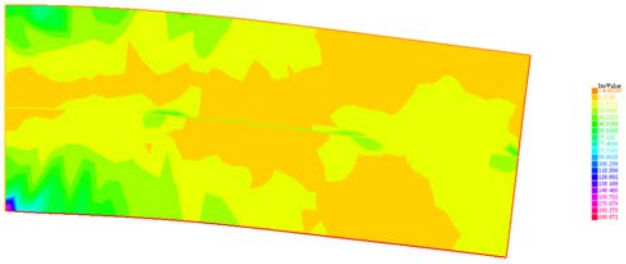

Fig. 5 Stress field of the clamped- free beam

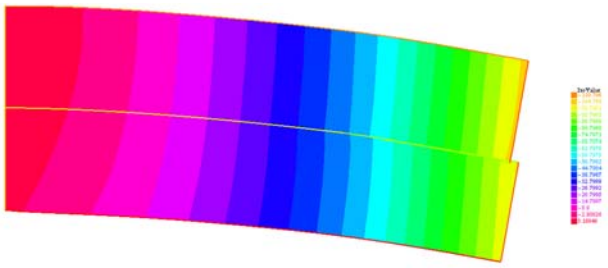

Fig. 6 Deflection field in the free end of the beam

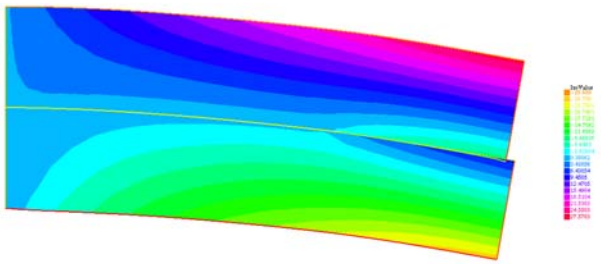

Fig. 7 Axial displacement in the free end of the beam

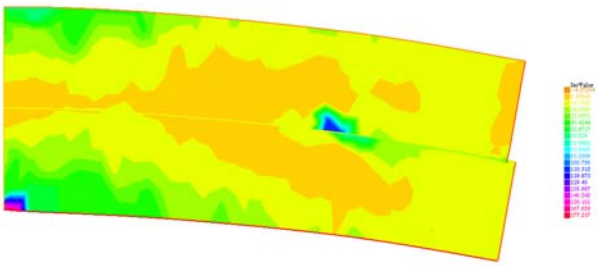

Fig. 8 Stress field in the free end of the beam

In the second example a delamination between the top and the bottom layers in the free end of the beam was considered. The delamination length is chosen to be $L_d = \frac{1}{3}L$. The material and geometric characteristics are the same as in the previous example problem.

Table 3 Natural frequencies for the clamped-free beam

Mode	$\nu(s^{-1})$ Exact	$\nu(s^{-1})$ Present model	Error (%)
1	84,5680793	84,5667407	8,03-05
2	354,439181	354,311628	0,007
3	932,529449	932,265657	0,01
4	1795,30077	1794,92573	0,02
5	2945,97338	2944,98303	0,05
6	4384,31414	4382,45853	0,11
7	6110,32306	6097,31073	0,78
8	8124,00013	8085,78424	2,29
9	10425,3454	10335,1917	5,40
10	13014,3587	12889,0197	7,52

Figs. 6 and 7 show the deflection field and the axial displacement field. Fig. 8 shows the stress field computed by this model for a clamped-free beam for the clamped-free beam.

Those figures show that the delamination appear between the top and the bottom layers. In the interfaces between the region with delamination and region without delamination appear some singularities and the stress field is higher in those interfaces compared to other region of the beam, which enables the location of the delaminationd.

The lowest 10 order natural frequencies computed with the present model are compared with the exact frequencies as shown in Table 3. Good agreement is observed between the two approaches, the differences of the 1st to the 10th order natural frequencies are less than 8%.

4. Conclusions

To investigate the behavior of the partially delaminated layers, a finite elements model of beam using the first-order shear deformation theory is used. Numerical results are presented for static and dynamic problems. The differences between the deflections computed from the present model and previously computed data show that the results agree very closely. The delamination appears in displacement and stress fields, which enables its location. The frequencies computed with the model based on the formulation presented in this paper are in good agreement with the exact results. This shows the validity of the assumptions adopted in the present paper.

References

Benzerga, D., Haddi, A. and Lavie, A. (2012), "Effect of natural load on delamination behaviour of a new hybrid woven composite", *Mechanika*, **18**(5), 503-507.

Brandt, F. (1998), "New load introduction concept for improved and simplified delamination beam testing", *Exp. Tech.*, **22**(1), 17-20.

Corigliano, A., Mariani, S. and Pandolfi, A. (2006), "Numerical analysis of rate-dependent dynamic composite delamination", *Compos. Sci. Technol.*, **66**(6), 766-775.

Coronado, P., Argüelles, A., Viña, J., Mollón, V. and Viña, I. (2012), "Influence of temperature on a carbon-fibre epoxy composite subjected to static and fatigue loading under mode-I delamination", *Int. J.*

Solid. *Struct*., **49**(21), 2934-2940.
Gőrkem, S.G. and Hűsem, M. (2013), "Ultimate behavior of composite beams with shallow I-sections", *Steel Compos*. *Struct*., *Int*. *J*., **14**(5), 493-509.
Greco, F. and Lonetti, P. (2009), "Mixed mode dynamic delamination in fiber reinforced composites", *Compos*. *Part B*: *Eng*., **40**(5), 379-392.
Hamed, M.A., Nosier, A. and Farrahi, G.H. (2006), "Separation of delamination modes in composite beam with symmetric delaminations", *Mater*. *Des*., **27**(10), 900-910.
Kim, S.H., Chattopadhyay, A. and Ghoshal, A. (2003), "Characterization of delamination effect on composite laminates using a new generalized layerwise approach", *Comput*. *Struct*., **81**(15), 1555-1566.
Lee, S., Park, T. and Voyiadjis, G.Z. (2002), "Free vibration analysis of axially compressed laminated composite beam-columns with multiple delaminations", *Compos*. *Part B*, **33**, 605-617.
Mahieddine, A., Pouget, J. and Ouali, M. (2010), "Modeling and analysis of delaminated beams with integrated piezoelectric actuators", *Comptes Rendus Mecanique*, **338**(5), 283-289.
Prokić, A., Lukić, D. and Ladjinović, Dj. (2014), "Automatic analysis of thin-walled laminated composite sections", *Steel Compos*. *Struct*., *Int*. *J*., **16**(3), 233-252.
Renart, J., Blanco, N., Pajares, E., Costa, J., Lazcano, S. and Santacruz, G. (2011), "Side Clamped Beam (SCB) hinge system for delamination tests in beam-type composite specimens", *Compos*. *Sci*. *Technol*., **71**(8), 1023-1029.
Sjögren, A. and Asp, L.E. (2002), "Effects of temperature on delamination growth in a carbon/epoxy composite under fatigue loading", *Int*. *J*. *Fatigue*, **24**(2-4), 179-184.
Zhang, J., Peng, L., Zhao, L. and Fei, B. (2012), "Fatigue delamination growth rates and thresholds of composite laminates under mixed mode loading", *Int*. *J*. *Fatigue*, **40**, 7-15.
Zhao, L., Gong, Y., Qin, T., Mehmood, S. and Zhang, J. (2013), "Failure prediction of out-of-plane woven composite joints using cohesive element", *Compos*. *Struct*, **106**, 407-416.

CC